



## WEDNESDAY SLIDE CONFERENCE 2018-2019

### Conference 13

2 January 2018

**Conference Moderator:**

Timothy Cooper, DVM, DACVP  
Pathology Department  
NIH/NIAID  
Integrated Research Facility  
Frederick, MD

---

**CASE I:** A-475-4 (JPC 4100984).

**Signalment:** 4-8 week old female  
C57BL/6NCrl mouse (*Mus musculus*)

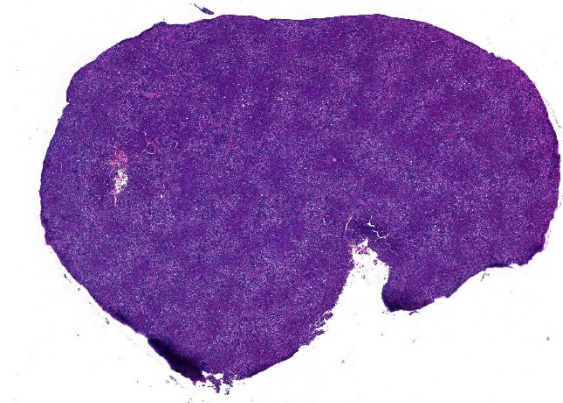
**History:** Experimentally infected with  
mouse adapted Ebola virus (ma-EBOV) by  
intraperitoneal route

**Gross Pathology:** Gross lesions included a  
pale and friable liver, pale kidneys, enlarged  
spleen and hemorrhagic/congested  
gastrointestinal tract

**Laboratory results:** N/A

**Microscopic Description:**

Slide contains a single section of liver. There  
is severe multifocal to coalescing  
predominantly periportal and midzonal  
hepatocellular degeneration and necrosis  
with moderate to severe mixed inflammation.



*Liver, mouse. There is a retiform pattern of hepatocellular necrosis evident at low magnification (HE,36X)*

In approximately 30% of lobules there is massive panlobular degeneration and inflammation. There is abundant periportal to midzonal microvesicular lipid type cytoplasmic vacuolation of hepatocytes, with frequent hyaline eosinophilic cytoplasmic inclusions (resembling Councilman bodies) and cell swelling. There are several foci of

hepatocyte dissociation and loss with acute hemorrhage. Apoptotic and necrotic hepatocytes are common. Small to large eosinophilic intracytoplasmic (viral) inclusions are present within viable and degenerate hepatocytes, Kupffer cells and rarely endothelial cells. Inflammatory cell infiltrate includes large numbers of macrophages and viable and degenerate neutrophils. Within central veins there are frequent vacuolated monocytes, occasionally with phagocytosed apoptotic debris or eosinophilic intracytoplasmic inclusions. There are scattered linear to branching fine olive green bile plugs within canaliculi between hepatocytes.

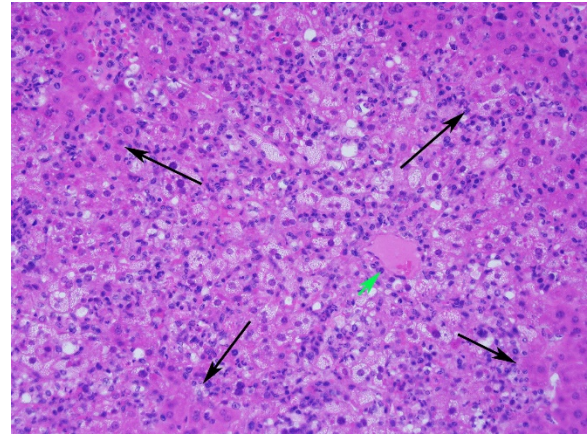
**Contributor’s Morphologic Diagnoses:**

Liver, hepatitis, necrotizing and histiocytic, multifocal to coalescing, acute, severe with intracytoplasmic inclusion bodies

**Contributor’s Comment:**

Liver lesions are severe and consistent with experimental mouse-adapted Ebola virus infection.<sup>2,3</sup> Ebola virus, a filovirus, is an important high consequence pathogen causing significant human disease, most recently a large outbreak in west Africa from 2014 to 2016, with a smaller outbreak in 2017. Ebola targets hepatocytes and Kupffer cells of the liver, resulting in widespread hepatocellular degeneration and necrosis. Liver lesions in human and non-human primate infections are conspicuous for the minimal to absent leukocytic infiltrate, in contradistinction to the lesion presented here.<sup>1,7</sup>

The extensive inflammation and absence of a distinct zonal (lobular/acinar) pattern point toward an infectious/inflammatory rather than toxic etiology. Not knowing the strain of mouse, immune status, experimental manipulation or other tissue lesions, reasonable differential etiologies for severe necrotizing hepatitis in a (usually



*Liver, mouse. There is diffuse vacuolar degeneration and widespread necrosis of centrilobular (central vein marked with a green arrow) and midzonal hepatocytes. . Portal areas re mildly vacuolated to morphologically normal (black arrows.) (HE, 200X)*

immunodeficient) mouse would include mouse hepatitis virus (MHV, type species of *Betacoronavirus*), mouse adenovirus (MAdV-1 or -2, *Mastadenovirus*), mouse cytomegalovirus (MCMV, *murid betaherpesvirus-1*, type species of *Muromegalovirus*), lymphocytic choriomeningitis virus (LCMV, type species of *Mammarenavirus*), or ectromelia virus (mousepox, *Orthopoxvirus*).<sup>1</sup> Mouse adenovirus and MCMV have intranuclear rather than intracytoplasmic inclusions, and mouse hepatitis virus lacks inclusions but forms characteristic syncytia. Ectromelia does form cytoplasmic inclusions in hepatocytes, but these tend to be difficult to visualize without prolonged hematoxylin staining. Viral cytoplasmic inclusions in hepatocytes must also be differentiated from phagocytosed neighboring apoptotic hepatocytes (Councilman bodies). Acute salmonellosis and Tyzzer’s disease would be additional differential etiologies, although the lesions tend to be more nodular, with intracellular bacterial stacks in the latter.<sup>1</sup>

**Contributing Institution:**

Pathology Department  
NIH/NIAID

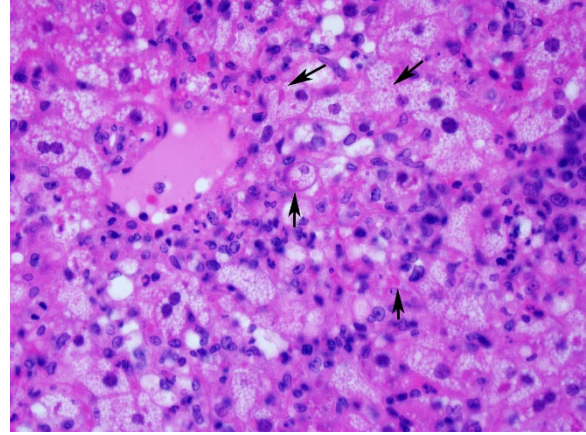
Integrated Research Facility

<https://www.niaid.nih.gov/about/integrated-research-facility>

**JPC Diagnosis:** Liver: Hepatitis, necrotizing and neutrophilic, random, diffuse, severe, with numerous intracytoplasmic viral inclusions.

**JPC Comment:** The first Ebola virus outbreak occurred in the Democratic Republic of the Congo (DRC) in 1976, resulting in 280 cases as a result of close contact and use of contaminated needles. A large outbreak in Western Africa from 2013-2015 claimed over 11,000 lives in multiple countries, with the majority of deaths in Sierra Leone, Liberia and Guinea with cases exported to other countries in Europe and North America for the first time.<sup>4</sup> At the time of this writing, another outbreak occurs in the DRC, with 130 confirmed cases. Outbreak control has been the key to the decreased in lives claimed by this disease over the last forty years, effective treatment and vaccination for this hemorrhagic fever of humans is still woefully inadequate.

The genus *Ebolavirus* is divided into five distinct species: Zaire ebolavirus (EBOV), Sudan ebolavirus, Tai Forest ebolavirus, Bundibugyo ebolavirus, and Reston ebolavirus (a species of ebolavirus that is fatal in macaques but not in humans.) The ebolaviruses can infect a number of animal species including non-human primates (chimpanzees, monkeys, macaques, orangutans, baboons), fruit bats, dogs, rodents, porcupines, and a range of laboratory rodents.<sup>4</sup> During human epizootics, bats have served as reservoirs in the source for infection. Bats are subclinical carriers, and do not show clinical signs of infection. Studies on arthropods have shown that they are not vectors of EBOV.<sup>4</sup>



*Liver, mouse. Degenerating hepatocytes contain one or more brightly eosinophilic intracytoplasmic viral protein inclusions (arrows). Moderate numbers of neutrophils infiltrate areas of necrosis. (HE,400X)*

Shortly after the initial outbreak in the DRC, nonhuman primate and guinea pig models were developed for infection with Zaire ebolavirus. The hemorrhagic fever seen in nonhuman primates closely resemble the human disease.<sup>2</sup> However the complications of working with nonhuman primate models, as well as their expense, demonstrated the need for the development of murine models. In addition, the possibility of using genetically engineered murine models to study specific cytokine interactions in a very complex viral pathogenesis further reinforced a call for development of an appropriate murine model. Ultimately, an appropriate murine model was eventually developed by passaging Zaire ebolavirus from the original outbreak through progressively older suckling mice until it could be transmitted to adult, immunocompetent BALB/c mice.<sup>2</sup>

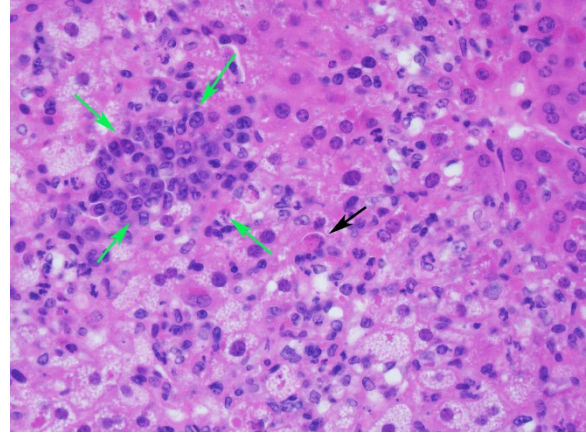
Mouse models such as the BALB/C share many similarities with guinea pig and NHPS models with cells of the mononuclear phagocyte system being target by the virus early in the disease. Viral replication may be seen in macrophages in lymph nodes and the spleen within 2 days of infection. On day three, when mice first show signs of clinical illness, virus replication is widespread, with



infection of hepatocytes, adrenocortical cells, fibroblasts, adipocytes, and cells of the monocyte-macrophage system in all organs. Histologic changes on day five include marked lymphocytolysis in multiple organs. Endothelial cell infection, even in late stages of disease, is uncommon. One notable difference in the mouse model as compared to humans and the NHP model is the noticeable paucity of fibrin thrombi within the spleen of infected mice (a very prominent finding in other model species as well as humans.)<sup>2</sup>

Since the development of the first murine model, flaws in the model have become apparent, as mouse models do not display other consequences of disease noted in humans, such as disseminated intravascular coagulation or death from shock, as seen in non-human primates. (An excellent 2015 article by Martines et al.<sup>5</sup> from the Centers for Disease Control and Prevention reviews the disease caused by ebolaviruses and the related Marburg virus in humans). Since that time, research in a wide variety of inbred mouse strains have identified resistant and susceptible strains and potentially responsible resistance genes which may reflect the apparent genetic susceptibility displayed in humans when a large population is infected by the virus.<sup>6</sup>

The moderator noted the difference between Ebola infections in mice and in primates, with the almost total lack of inflammatory cells within primate specimens. Ebola is not a virus that can be simply injected in mouse models – it is serially passaged, and mouse-adapted strains need to be injected IP for infection. He also discussed the peculiar abnormalities associated with C57BL/6N strains, including retinal dysplasia, and if they are 6Nhsd, a mutation which causes an impaired immune response.



*Liver, mouse. Apoptotic hepatocytes are rounded up and individualized. An aggregate of immature granulocytes (extramedullary hematopoiesis) is present at upper left (green arrows) (HE, 400X)*

The moderator cautioned about over interpreting the lipid change in this particular animal – it may be quite variable based on time of day, elapsed time since last meal, and in sick mice, inability to feed.

#### References:

1. Barthold, S.W., S.M. Griffey, and D.H. Percy, *Mouse*, in *Pathology of Laboratory Rodents and Rabbits*, S.W. Barthold, S.M. Griffey, and D.H. Percy, Editors. 2016, Wiley Blackwell: Ames, IA. p. 1-118.
2. Bray M, Davis K, Geisbert T, Schmaljohn C, Huggins J. A mouse model for evaluation of prophylaxis and therapy of Ebola hemorrhagic fever. *J Infect Dis* 1998; 178(3): 651-61.
3. Gibb TR, Bray M, Geisbert TW, Steele KE, Kell WM, Davis KJ, Jaax NK. Pathogenesis of experimental Ebola Zaire virus infection in BALB/c mice. *J Comp Pathol* 2001. 125(4):233-42.
4. Gumusova S, Sunbul M, Lebecicioglu. Ebola virus disease and the veterinary perspective. *Ann Clin Microbiol and Antimicrobials* 2015; 14:30-35.

5. Martines RB, Ng DL, Greer PW, Rollin PE, Zaki SR. Tissue and cellular tropism, pathology and pathogenesis of Ebola and Marburg viruses. *J Pathol* 2015. 235(2):153-74.
6. Rasmussen AL, Okumura A, Ferris MT, Green R, Feldmann F, Kelly SM, Scott DP, Safronetz D, Haddock E, LaCase R, Thomas MJ, Sova P, Carter VS, Weiss JM, Miller DR, Shaw GD, Korth MJ, Heise MY, Baris RS, deVilena FPD, Feldmann H, Katze MG. Host genetic diversity enables Ebola hemorrhagic fever pathogenesis and resistance. *Science* 2014; 346(6212):987-991.
7. Ryabchikova, E.I., L.V. Kolesnikova, and S.V. Luchko, An analysis of features of pathogenesis in two animal models of Ebola virus infection. *J Infect Dis* 1999; 179 Suppl 1: S199-202.

**CASE II: N1301/17B: (JPC 4105937).**

**Signalment:** 4.5 years, male-neutered, Domestic Shorthaired, *Felis catus*, cat

**History:** A 4.5 year-old male-neutered cat was submitted to post mortem examination. Found dead unexpectedly.

**Gross Pathology:** The cat weighed 4.5 kg and was in a good body condition with adequate subcutaneous and intraabdominal fat deposits. Skeletal musculature of both hind limbs was mottled pale to red. The thoracic cavity contained 30 ml of translucent serosanguinous fluid. The trachea contained moderate amounts of white froth and both lungs were diffusely heavy and wet with copious frothy fluid on cut surface. The heart weighed 35g and the left atrium was subjectively enlarged. The left to right free ventricular wall ratio was 3:1 (9:3 mm). The septum measured 9 mm in thickness. Located

at the aortic bifurcation was a 3 cm plug of friable dark red to tan material, completely occluding the vessel lumen and extending along both iliac arteries. Thyroid glands were bilaterally unremarkable.

**Laboratory results:** None.

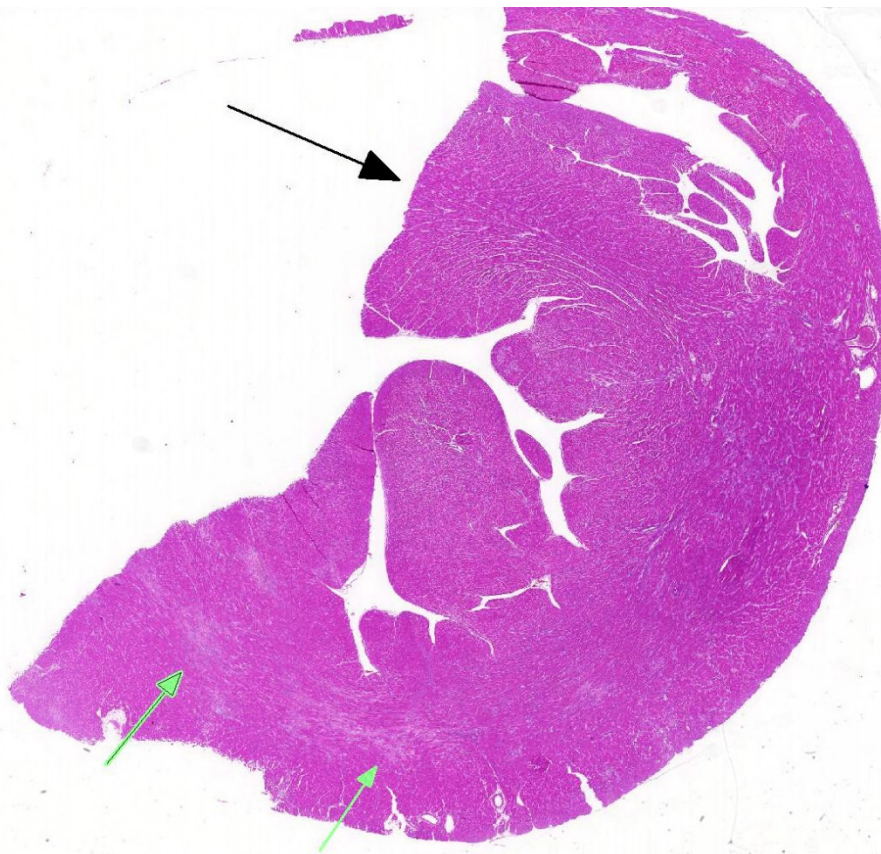
**Microscopic Description:**

**Heart:** Affecting approximately 10-20% of the myocardium of the left ventricular free wall are broad bands of mature and developing fibrous tissue extensively replacing and dissecting between cardiac myocytes. Myocytes entrapped within fibrous tissue are often shrunken and hypereosinophilic and have lost cross-striation (segmental degeneration). Fibrosis affects mainly the middle aspect of the left free ventricular wall and smaller foci within the septum. Furthermore, cardiac myocytes of the left ventricle are multifocally arranged in an interwoven pattern (myofiber disarray). Within the left ventricular wall and extending into the right ventricular wall, myocytes frequently measure 2-3 times normal diameter and show vesicular nuclei (hypertrophy).

**Contributor's Morphologic Diagnoses:**

**Heart:** Hypertrophic cardiomyopathy, domestic shorthaired cat, *Felis catus*.

**Contributor's Comment:** Hypertrophic cardiomyopathy (HCM) is the most frequent feline cardiomyopathy, accounting for almost two thirds of cases.<sup>3</sup> In affected cats, a thickened and remodeled ventricular cardiac muscle, unable to relax completely during diastole, leads to incomplete ventricular filling and thus a decreased preload (diastolic dysfunction).<sup>2</sup> Common clinical signs include lethargy, heart murmurs, tachycardia and/or may be secondary to pulmonary oedema (dyspnea, coughing) or



*Heart, cat. A cross section of heart at the level of the papillary muscle is submitted. The left ventricular free wall and interventricular septum (black arrow) is thickened. There are multiple areas of myocardial fibrosis (green arrows) visible at subgross magnification. (HE, 5X)*

thromboembolism (hindlimb paresis).<sup>1,3,9</sup> Sudden death may also occur.<sup>1</sup>

This case illustrates classical features of idiopathic feline HCM, including subsequent aortic thromboembolism. At 35g, the heart was markedly heavier than normal in adult cats (<20-25g) and within the upper range of values reported for cats that died of HCM (29-37g).<sup>2</sup> As in the present case, symmetrical and concentric hypertrophy of the myocardium is most common, thus retaining a 'normal' left:right ventricular free wall ratio of 3:1, while wall thicknesses are absolutely increased.

Alterations in blood flow and velocity, especially within the often dilated left atrium, may lead to turbulence and produce focal thrombi, which may subsequently be flushed

into circulation, where they become lodged most frequently at the aortic-iliac junction.<sup>9</sup> At this location, thromboembolism leads to acute hindlimb paraparesis with clinical signs classically termed the five 'p's' (paresis-pain-pallor-pulselessness-poikilothermy), which may be the first presenting clinical sign of a cat with HCM.<sup>10</sup> Renal cortical infarcts may also be a feature indicating previous thromboembolism of renal arteries (not present in this case).

Histological hallmarks of feline HCM are hypertrophied cardiac myocytes with vesicular nuclei, myofiber disarray, especially within the left free ventricular wall and septum, and replacement fibrosis, all of which can be observed in this case.<sup>9</sup> Further, medial hypertrophy of intramyocardial arteries with or without perivascular mononuclear infiltrates may be present.<sup>9</sup> If performed antemortem, immunoassays for cardiac biomarkers often reveal increased levels of cardiac troponin I, indicating ongoing myocardial damage.<sup>4</sup> A familial predisposition for HCM is best characterized in the Maine Coon and Ragdoll breeds.<sup>7,8</sup> Two separate mutations have been identified affecting the gene coding for myosin binding protein C3 (MYBPC3): an alanine for proline substitution in exon 3 of the MYBPC3 gene



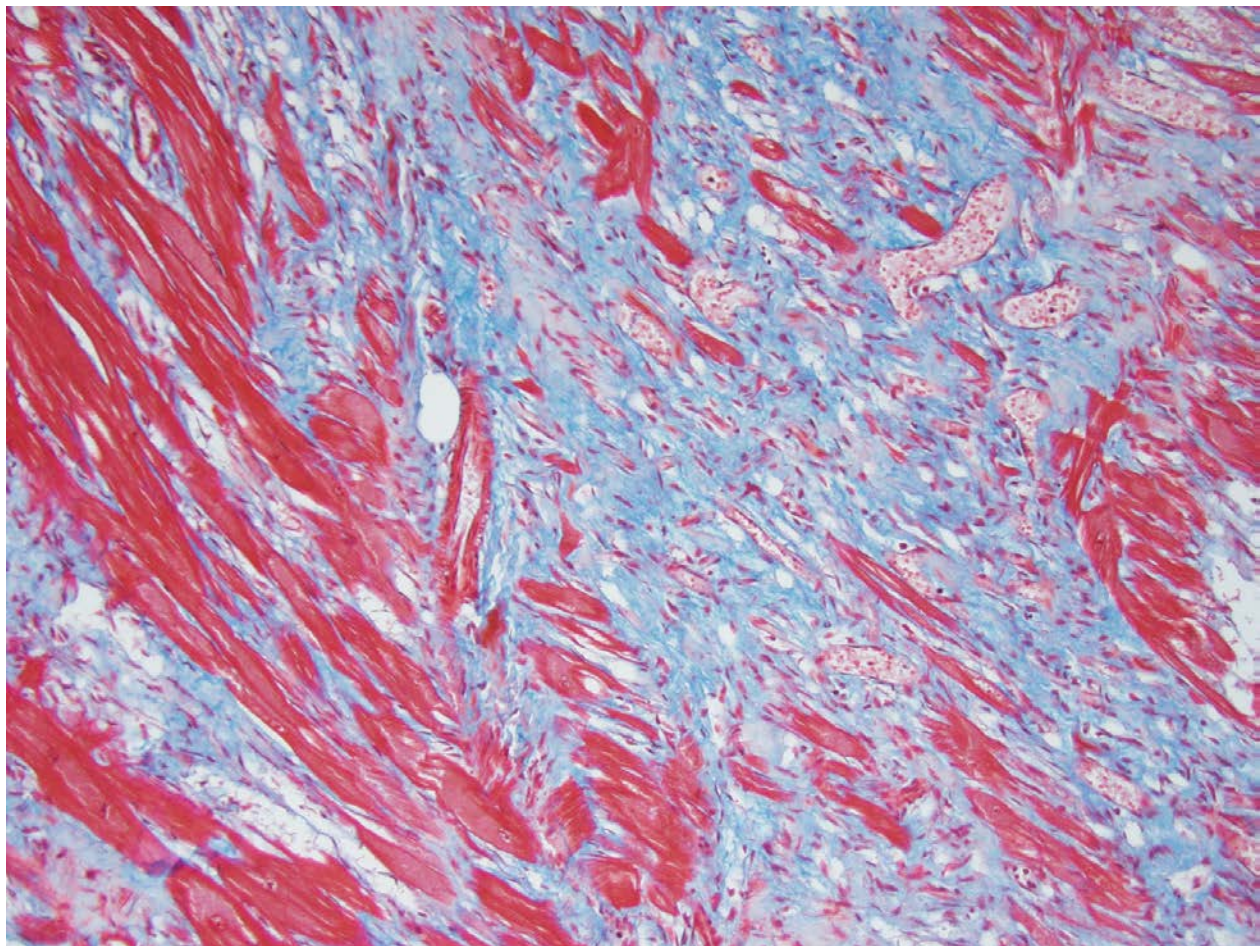




similar case exists in Maine Coon cats, as not all affected individuals demonstrate known mutations.<sup>1</sup>

Cardiac troponin I (cTnI) is commonly used as a measurement for ongoing myocardial damage in cats (and humans) with HCM; this protein, which inhibits the structural interaction of the myosin heads with the actin-binding sites in cardiac and skeletal muscle, has been shown to increase rapidly in the serum after cardiomyocyte injury and is a sensitive and specific marker for cats with moderate to severe HCM as compared to normal cats whether or not congestive heart failure is present. Although there is still some debate, increased levels of cTnI are generally consistent with irreversible myocardial damage.<sup>5</sup>

One of the characteristic histologic changes associated with HCM is cardiomyocyte loss and fibrosis, which often starts in proximity to myocardial vessels. A number of vascular changes have been identified in cats and humans with HCM, to include microvascular or intramural coronary arterial disease, which likely result in areas of ischemic damage and resulting fibrosis, initially localized to perivascular areas within the myocardium.<sup>5</sup> In humans with HCM, abnormal coronary flow dynamics, decreased coronary artery diastolic reserve, and systolic compression of the septal perforator arteries have been documented as contributory to myocardial ischemia. Furthermore, the increase in myocardial muscle mass without compensatory increase in myocardial



*Heart, cat. A Masson's trichrome demonstrates the areas of fibrosis as blue against the red background of viable myocardium. (HE, 320X)*



capillary density is also likely to contribute to ischemic damage in the myocardium of affected individuals.<sup>4</sup>

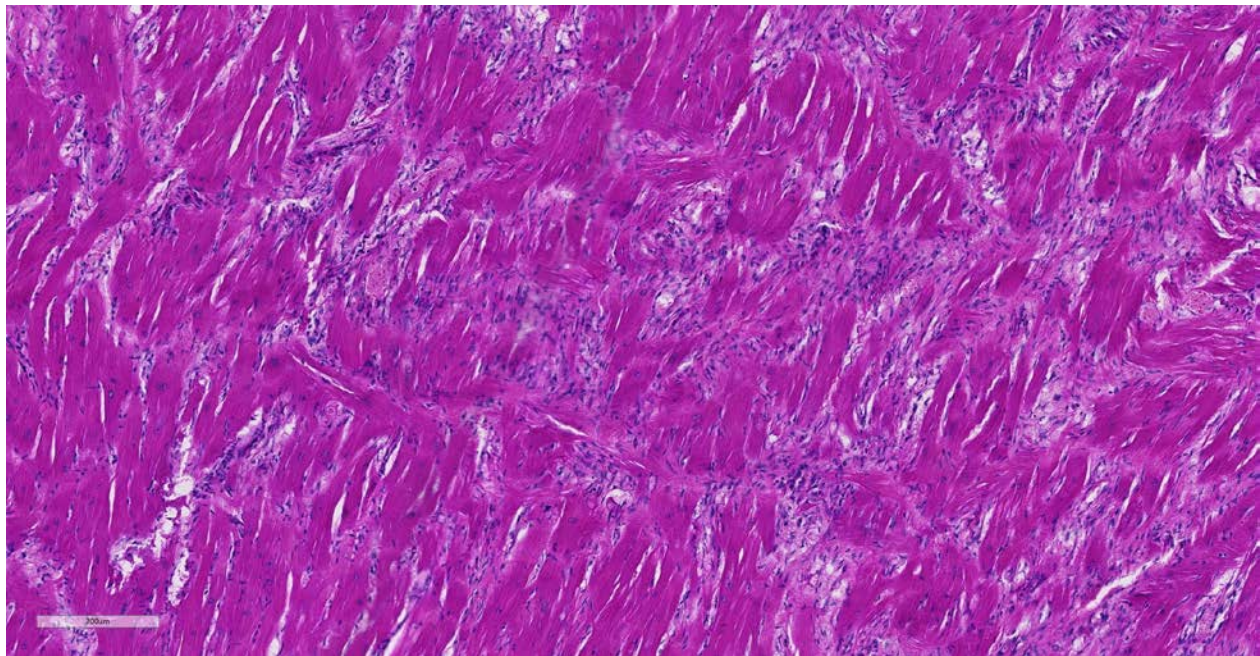
Since 1960, surgical intervention and septal myomectomy have been common approaches to relieving left ventricular outflow tract obstruction. Alcohol septal ablation (a less invasive procedure in which ethanol is injected to the first or second perforator artery, resulting in localized myocardial infarction) was introduced in 1994, and its surgical complication rate has proven to be similar to that of surgical myomectomy.<sup>4</sup>

During the conference, the moderator cautioned about interpretation of luminal diameter in these cases, based on a lack of knowing the level of section within the heart as well as the status of rigor during fixation.

In the normal heart, myofibers are often maloriented to each other at the area in which ventricles meet the interventricular septum – this may be misinterpreted. The described

feature of ‘myofiber disarray’ in HCM is most appropriately evaluated wholly within the left ventricular free wall or septum. In cases of microscopic examination of the heart, it would be unusual to be able to take a cross=section through the ventricles and septum and not find disarrayed fiber, but emphasized the need to take multiple sections to completely evaluate the heart. Without the presence of the disarrayed fibers, a diagnosis of HCM cannot be made; the hypertrophic changes seen in a number of fibers such as markedly enlarged nuclei are non-specific and may be seen in a number of heart diseases.

Microscopically, the moderator briefly discussed the differentiation between “interstitial” and “replacement” fibrosis for complete description of this lesion, and highlighted the need for a Masson’s trichrome to fully appreciate the amount of fibrosis in this case.



*Heart, cat. Within the left ventricle of this section, there is a large focal area in which myofibers assuming an interlacing “basket-weave” appearance. (HE, 320X)*

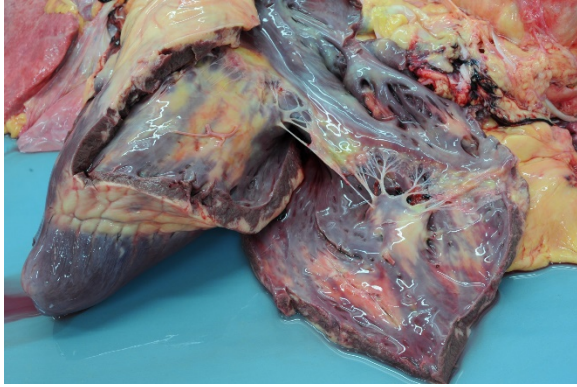
## References:

1. Abbott JA. Feline hypertrophic cardiomyopathy: an update. *Vet Clin North Am Small Anim Pract* 2010; 40(4):685-700.
2. Côté E, MacDonald KA, Meurs KM, Sleeper MM. *Feline Cardiology*. 1st ed. Wiley-Blackwell, West Sussex, UK, 2011:110-112.
3. Ferasin L, Sturgess CP, Cannon MJ, Caney SM, Gruffydd-Jones TJ, Wotton PR. Feline idiopathic cardiomyopathy: a retrospective study of 106 cats (1994-2001). *J Feline Med Surg* 2003; 5(3):151-159.
4. Hang DH, Nguyen A, Schaff HY. Surgical treatment of hypertrophic cardiomyopathy: a historical perspective. *Ann Cardiothor Surg* 2017; 6(4):318-328.
5. Herndon WE, Kittleson MD, Sanderson K, Drobatz KJ, Clifford CA, Gelzer A, Summerfield NJ, Linde A, Sleeper MM. Cardiac troponin I in feline hypertrophic cardiomyopathy. *J Vet Intern Med* 2002; 16(5):558-564.
6. Kittleson MD, Meurs K, Harris S. The genetic basis of hypertrophic cardiomyopathy in cats and humans. *J Vet Cardiol* 2015; 17(Suppl 1):S53-S73.
7. Liu SK, Peterson ME, Fox PR: Hypertrophic cardiomyopathy and hyperthyroidism in the cat. *J Am Vet Med Assoc* 1984; 185(1):52-57.
8. Meurs KM, Fox PR, Magnon AL, Liu S, Towbin JA. Molecular screening by polymerase chain reaction detects panleukopenia virus DNA in formalin-fixed hearts from cats with idiopathic cardiomyopathy and myocarditis. *Cardiovasc Pathol* 2000; 9(2):119-126.
9. Meurs KM, Norgard MM, Ederer MM, Hendrix KP, Kittleson MD. A substitution mutation in the myosin binding protein C gene in ragdoll hypertrophic cardiomyopathy. *Genomics* 2007; 90(2):261-264.
10. Meurs KM, Sanchez X, David RM, Bowles NE, Towbin JA, Reiser PJ, Kittleson JA, Munro MJ, Dryburgh K, Macdonald KA, Kittleson MD. A cardiac myosin binding protein C mutation in the Maine Coon cat with familial hypertrophic cardiomyopathy. *Hum Mol Genet*; 2005 14(23):3587-3593.
11. Robinson WF, Robinson NA. Cardiovascular System. In: Maxie MG, ed. *Jubb, Kennedy and Palmer's Pathology of Domestic Animals*. 6th ed. Elsevier, St. Louis, MO, USA, 2016:46-47.
12. Smith SA, Tobias AH. Feline arterial thromboembolism: an update. *Vet Clin North Am Small Anim Pract*; 2004; 34(5):1245-1271.

### CASE III: 317048 (JPC 4033739).

**Signalment:** 15-year-old, Clydesdale-Cob cross, male castrated, horse (*Equus caballus*).

**History:** The animal presented to the Weipers Centre at the University of Glasgow for re-evaluation of episodes of syncope that had been noted sporadically over the preceding two years. The horse had been investigated for syncope associated with polycythaemia and elevation of cardiac



*Heart, horse. Grossly, the right ventricular wall is multifocally and rarely transmurally infiltrated by fat; similar changes are seen in the interventricular septum as well. (Photo courtesy of: Veterinary Diagnostic Services, School of Veterinary Medicine, College of Medical, Veterinary and Life Sciences, University of Glasgow, Bearsden Road, G61 1QH, Glasgow, United Kingdom, [www.glasgow.ac.uk/vds](http://www.glasgow.ac.uk/vds))*

troponin (CTnI). Cardiac dysrhythmias had resolved over time, with correction of red cell count and CTnI levels. Since then, the horse had returned to ridden exercise with no observed collapses until one week before presentation when it went down into lateral recumbency, paddled with his front legs and chomped his lips, appearing to have lost consciousness, the eyes appeared vacant and the horse remained down for two to three minutes after which he recovered and appeared normal. On presentation the horse was bright and alert and in good body condition (613kg). The syncopal episodes had implications for horse welfare and human safety, therefore the owner elected euthanasia.

**Gross Pathology:** On macroscopic examination, the epicardium of the right ventricular free wall was replaced by a yellowish soft material that expanded extensively from the coronary arteries towards the center of the ventricle and was also multifocally distributed in small foci within the remaining myocardial fibers, which accounted for less than 40% of the total right ventricle. Upon opening the right ventricle, the endocardium was similarly

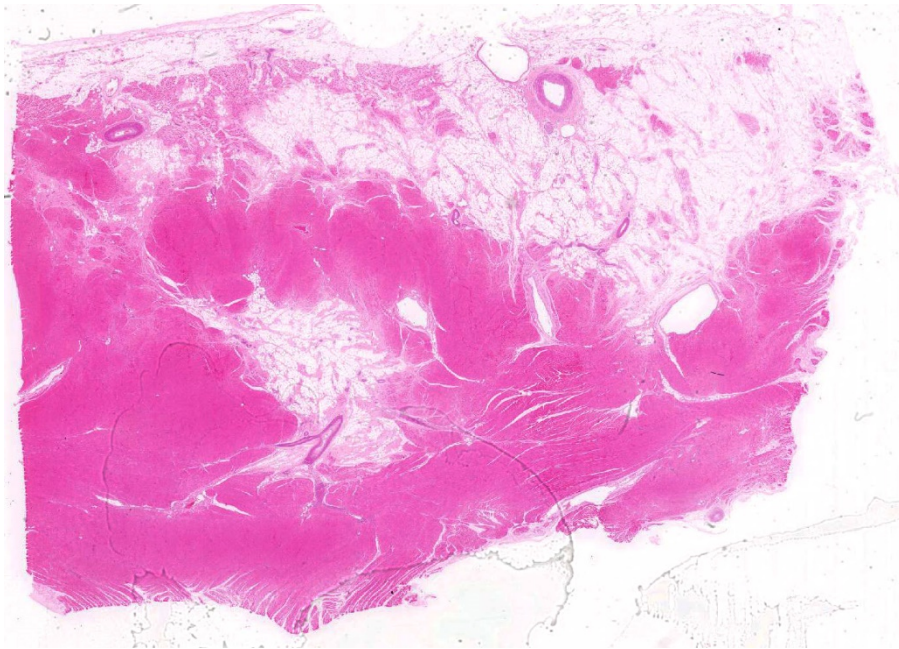
replaced by this abnormal tissue extending multifocally up to 1cm deep into the myocardium from both the epicardium and endocardium. The left ventricle was similarly affected, with approximately 20% of the myocardial tissue being replaced by yellowish soft tissue. Small foci of this yellowish tissue were also multifocally observed in both the left and right atria. No other significant gross pathologic findings were observed in other organ systems.

**Laboratory results:** Haematology and biochemistry profiles were unremarkable. Serum amyloid A and fibrinogen were within normal limits. CTnI was within reference range. On ECG examination there were multiple short periods of sinus tachycardia with no apparent external stimuli and also one episode of profound tachycardia, four ventricular premature complexes were also present. Echocardiography and neurological evaluation were unremarkable.

#### **Microscopic Description:**

Microscopic findings were similar in both ventricles, being more extensive in the right ventricular free wall; and similar to those previously described in horses. Cardiomyocytes extensively within subepicardial zone and multifocally within the myocardial and subendocardial areas are markedly reduced in number and replaced by abundant adipose tissue intermixed with variably thickened bundles of fibrous connective tissue. Residual cardiomyocytes within the adipose tissue or surrounding it are highly vacuolated, and often with loss of myofibrils and nuclear detail (degeneration). Interspersed within the fibrous and adipose tissue infiltrate are low numbers of mononuclear inflammatory cells, mainly lymphocytes and macrophages. Periodic acid-Schiff (PAS) stain highlighted the disruption of Purkinje fibres by adipose tissue. Masson's trichrome stain highlighted





*Heart, horse. The epicardium (at top) and the myocardium in subepicardial and superficial myocardium is infiltrated by well-differentiated adipocytes. (HE, 6X)*

the variably thickened bundles of fibrous connective tissue dissecting the myofibers.

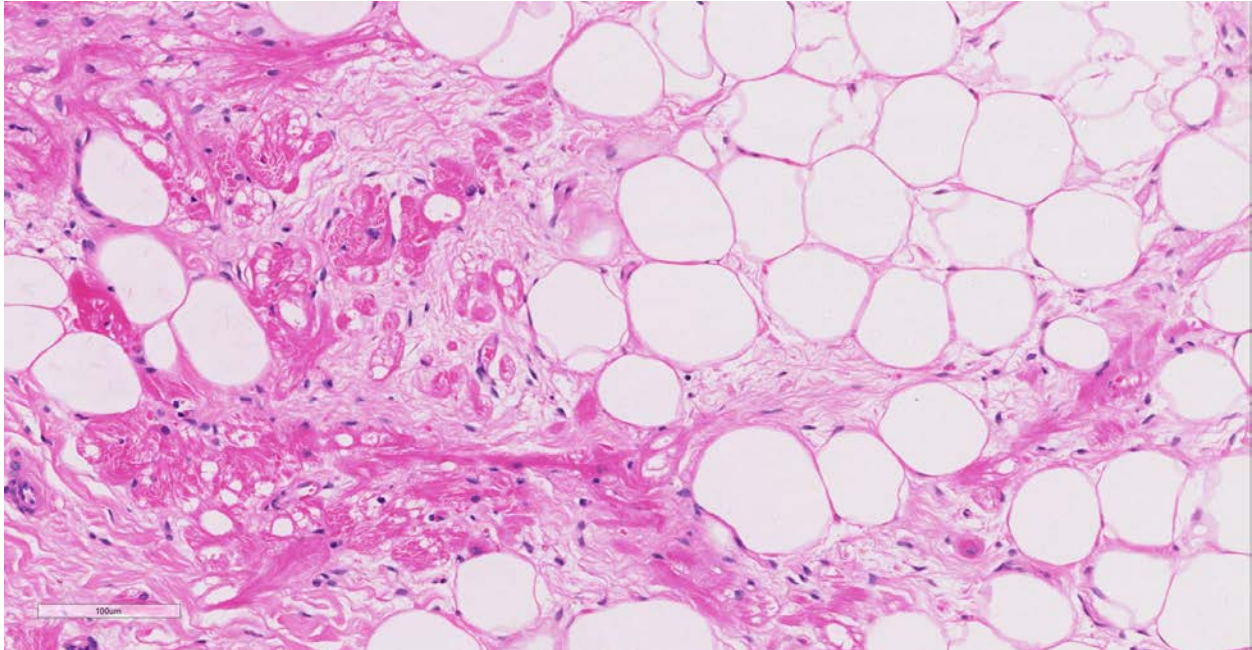
**Contributor's Morphologic Diagnoses:** Myocardial degeneration, focally extensive, severe, chronic; with marked adipose tissue replacement with fibrosis, myocardium, Clydesdale-Cob cross, male castrated, horse (*Equus caballus*).

**Contributor's Comment:** Arrhythmogenic right ventricular cardiomyopathy is a well-recognized entity in human beings from which clinicopathological features were described in 1982.<sup>5,15</sup> The condition has also been described in Boxer dogs<sup>1,6</sup> and cats<sup>2</sup> with similar gross and histological appearances; reports of this similar condition in breeds of dogs other than Boxer has also been described.<sup>9</sup> Recently, a similar condition was diagnosed in two horses<sup>3</sup> that died with no previous signs and in which both hearts were bearing fibro-fatty replacement similar to the case we present here.

While the two previous equine cases died without showing clinical signs, in this case there is a prolonged history of collapse and cardiac dysrhythmias. Young human cases are presented most commonly with cardiomegaly, congestive heart failure or sudden death<sup>5,14</sup> while adult patients usually have a more extensive history of recurrent ventricular arrhythmias and ventricular

tachycardia.<sup>5</sup> Clinical signs in Boxer dogs vary widely from sudden death to congestive heart failure with or without arrhythmias<sup>6</sup> while cats usually do not present any signs of arrhythmia and die due to congestive heart failure.<sup>2</sup>

This cardiomyopathy is a human familial condition of autosomal dominant inheritance with various degrees of penetrance.<sup>4</sup> Mutations in genes involved in cell adhesion complexes such as desmoglein-2 (GSG2) or plakophilin-2 (PKP2) have been found to be associated with ARVC in humans<sup>1</sup>, which supports the hypothesis that this condition is caused by inadequate cell-to-cell adhesion between cardiac myofibers leading to detachment of cardiomyocytes, cell death and replacement by adipose tissue with fibrosis.<sup>4</sup> Several desmosomal genes and the cardiac ryanodine receptor (RyR2) gene (involved in excitation-contraction coupling across the ventricles and mutated in some unique forms of human ARVC) have been investigated in boxer dogs with no positive



*Heart, horse. The myocardium is multifocally infiltrated by well-differentiated adipocytes (right), as well as poorly cellular fibrous connective tissue. Entrapped and degenerating cardiomyocytes contain large clear vacuoles, and are often shrunken and hyalinized (atrophy). (HE 181X)*

relationship established.<sup>7,8,16</sup> This could be, however, due to the substantial genetic heterogeneity of the disease.

With only three cases reported in horses, it is difficult to determine correlation between sex, age or exercise. However, the three cases were all male horses of heavy breeds (Clydesdale and Cob) in the same geographic region, which could possibly indicate a genetic relationship as is observed in many human cases.<sup>14</sup>

**Contributing Institution:**

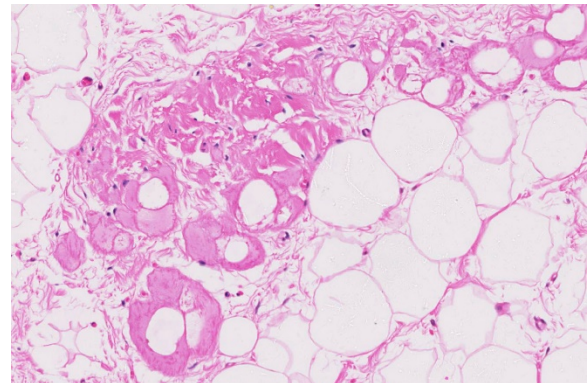
Veterinary Diagnostic Services, School of Veterinary Medicine  
 College of Medical, Veterinary and Life Sciences, University of Glasgow  
 Bearsden Road  
 G61 1QH  
 Glasgow, United Kingdom  
[www.glasgow.ac.uk/vds](http://www.glasgow.ac.uk/vds)

**JPC Diagnosis:**

Heart, ventricle: Fibrofatty infiltration, subepicardial and myocardial, multifocal to coalescing, severe, with cardiomyocyte, atrophy, and loss.

**JPC Comment:**

The uncommon syndrome of humans and Boxer dogs (often referred to as “Boxer cardiomyopathy”) of arrhythmogenic right ventricular cardiomyopathy is poorly named, as the evolving literature has identified cases



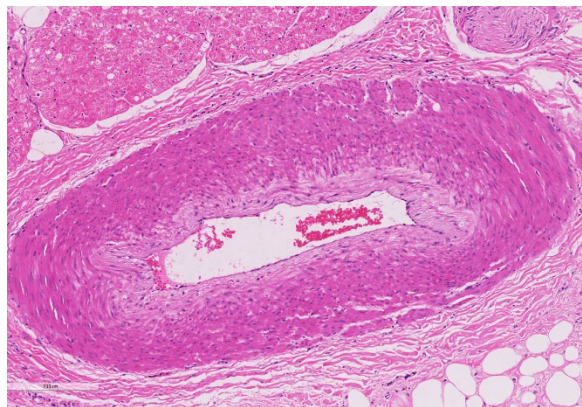
*Heart, horse. Entrapped Purkinje fibers also contain large clear cytoplasmic vacuoles. (HE, 282X)*



in which degenerative lesions (and subsequent generation of arrhythmias) may arise in the atria and frequently, the left ventricle.

While mutations in several desmosomal genes have been identified as causative in the human condition, and a loss of desmosomal integrity has been identified in affected Boxers, mutations of desmosomal genes have not yet been identified in the Boxer model.<sup>10</sup> Striatin, a scaffolding protein localized to intermediate filaments and the intercalated disk has been proposed as a potential cause in the Boxer. Decreased Wnt signaling in the myocardium of genetically engineered mouse models of ARVC appears to be responsible for increased myocardial adipogenesis, stimulating abnormal cell proliferation and differentiation as a result of beta-catenin accumulation in the cytoplasm of cardiac progenitor cells. Abnormal levels of beta catenin and mislocalization of this protein as well as striatin have been identified in affected Boxers.<sup>10</sup>

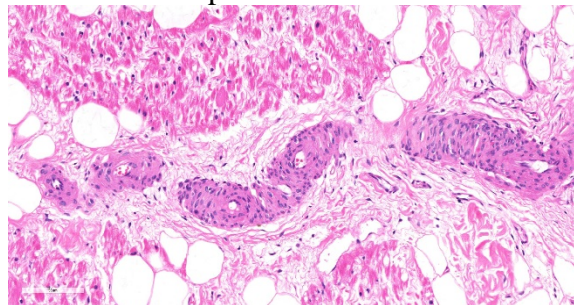
The veterinary literature is sparse with regard to this entity in the horse. This particular case was reported in the literature in 2015<sup>12</sup>, bringing the total number of reported equine cases to three. In previous studies of cardiac muscle in several equine populations, including racing, working, and a general



*Heart, horse. There is subintimal fibrosis of intramyocardial coronary arteries. (HE, 128X)*

population, fibrofatty infiltration has not been identified as a post-mortem finding. Similar changes were noted within the right ventricle of the two other reported equine cases.<sup>12</sup> The microscopic changes noted in this entrapped myofibers are also commonly seen in the human cases, to include cytoplasmic vacuolation and nuclear dysmorphism.<sup>11</sup>

ARVC has also been reported in two related chimps in a zoo collection (14 and 16 years of age) with no premonitory signs. A predominance of fibrofatty infiltration over the traditional interstitial fibrosis of the so-called “fibrosing cardiomyopathy”, considered the predominant form of heart disease in this species.<sup>17</sup>



*Heart, horse. There is multifocal mural smooth muscle hyperplasia of intramyocardial arterioles. (HE, 128X)*

A number of questions remain about the pathophysiology of this fascinating disease. Why are changes most prominent in the right ventricle? Current theory points to the thin wall and increased distensibility of the right ventricle which predisposes it to desmosomal failure;<sup>13</sup> the identified cases of ARVC involving the atria as well as left ventricle does not put this pathogenesis into dispute. There is dispute within the literature as to whether the lesion is the result of abnormal proliferation or an aberrative repair response – earlier studies such as the one in the feline model of ARVC identified a much higher number of cases with myocardial inflammation to a level not identified in other models<sup>2</sup>; their association of inflammation and fibrofatty repair was made prior to



identification of causative genes in human cases and generation of genetically engineered mouse models.

## References:

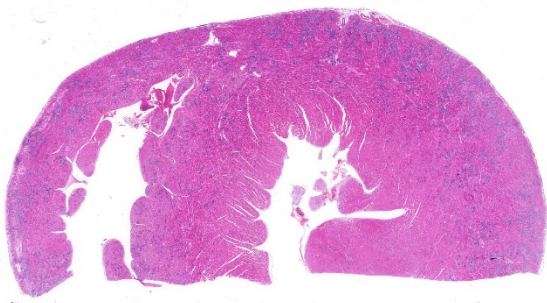
1. Basso C, Fox PR, Meurs KR. Arrhythmogenic right ventricular cardiomyopathy causing sudden cardiac death in Boxer dogs: a new animal model of human disease. *Circulation* 2004; 109:1180-1185.
2. Fox PR, Maron BJ, Basso C.. Spontaneously occurring arrhythmogenic right ventricular cardiomyopathy in the domestic cat: A new animal model similar to the human disease. *Circulation* 2000; 102:1863-1870.
3. Freel KM, Morrison LR, Thompson H, et al. Arrhythmogenic right ventricular cardiomyopathy as a cause of unexpected cardiac death in two horses. *Veterinary Record*. 2010; 166:718-722.
4. Kies P, Bootsma M, Bax J, et al. Arrhythmogenic right ventricular dysplasia/cardiomyopathy: Screening, diagnosis and treatment. *Heart Rhythm*. 2006; 3(2):225-234.
5. Marcus FI, Fontain GH, Guiraudon G. . Right ventricular dysplasia: a report of 24 adult cases. *Circulation*. 1982; 65: 384-398.
6. Meurs KM, Spier AW, Miller MW. Familial ventricular arrhythmias in boxers. *J Vet Intern Med*. 1999; 13:437-439.
7. Meurs KM, Lacombe VA, Dryburgh K, et al. Differential expression of the cardiac ryanodine receptor in normal and arrhythmogenic right ventricular cardiomyopathy canine hearts. *Hum Genet* 2006; 120:111–118.
8. Meurs KM, Erderer MM, Stern JA, et al. Desmosomal gene evaluation in Boxers with arrhythmogenic right ventricular cardiomyopathy. *Am J Vet Res*. 2007; 68(12):1338-1341.
9. Nakao S, Hirakawa A, Yamamoto S, et al. Pathologic features of arrhythmogenic right ventricular cardiomyopathy in middle-aged dogs. *J Vet Med Sci* 2011; 73(8):1031-6.
10. Oxford EM, Danko CG, Fox PR, Kornrich BG, Moise NS. Change in beta catenin localization suggests involvement of the canonical Wnt pathway in Boxer dogs with arrhythmogenic right ventricular cardiomyopathy. *J Vet Intern Med* 2014; 28:92-101.
11. Pilichou K, Nava A, Basso C, et al. Mutations in Desmoglein-2 Gene Are Associated With Arrhythmogenic Right Ventricular Cardiomyopathy. *Circulation*. 2006; 113:1171-1179.
12. Raftery AG, Garcin NC, Thompson HT, Sutton DGM. Arrhythmogenic right ventricular cardiomyopathy secondary to adipose infiltration as a cause of episodic collapse in a horse. *Irish Vet J* 2015;68:24. Doi 10.1186/s13620-015-0052-3.
13. Sen-Chowdry S, Morgan RD, Chamber JC. Arrhythmogenic cardiomyopathy: etiology diagnosis, and treatment. *Ann Rev Med* 2010; 61:233-253.
14. Thiene G, Nava A, Corrado D, et al. Right ventricular cardiomyopathy and sudden death in young people. *N Engl J Med*. 1988; 318(3):129-133.
15. Thiene G, Basso C. Arrhythmogenic right ventricular cardiomyopathy: An update. *Cardiovascular pathology*. 2001; 10:109-117.
16. Tiso N, Stephan DA, Nava A, et al. Identification of mutations in the cardiac ryanodine receptor gene in families affected with arrhythmogenic right ventricular cardiomyopathy type 2 (ARVC2). *Human molecular genetics*. 2001; 10(3):189-194.

17. Tong LJ, Flach EJ Sheppard MN, Pocknell A, aenerjee AA, Boswood A, Bouts T, Routh A, Feltre. Fatal Arrhythmogenic right ventricular cardiomyopathy in two related subadult chimpanzees (*Pan troglodytes*). *Vet Pathol* 2014; 51(4): 858-887.

**CASE IV: 317048 (JPC 4033739).**

**Signalment:** 2-year and 6-month old female neutered domestic shorthair cat (*Felis catus*)

**History:** The animal was presented to the Internal Medicine department of the University Small Animal Hospital in the University of Glasgow School of Veterinary Medicine. The animal had a 6 week history of pica (licking coal) with a more recent history of reduced appetite and lethargy culminating to progressive deterioration of body condition. The animal was again referred to the Small Animal Hospital of the University and found to be tachypnoeic and lethargic. An echocardiogram showed thickening of the left ventricular wall and interventricular septum, mild pericardial effusion and a moderate pleural effusion. 45ml of blood tinged fluid was drained from the thorax. The fluid had a high protein count with clotting protein noted within the syringes. The respiratory rate improved but



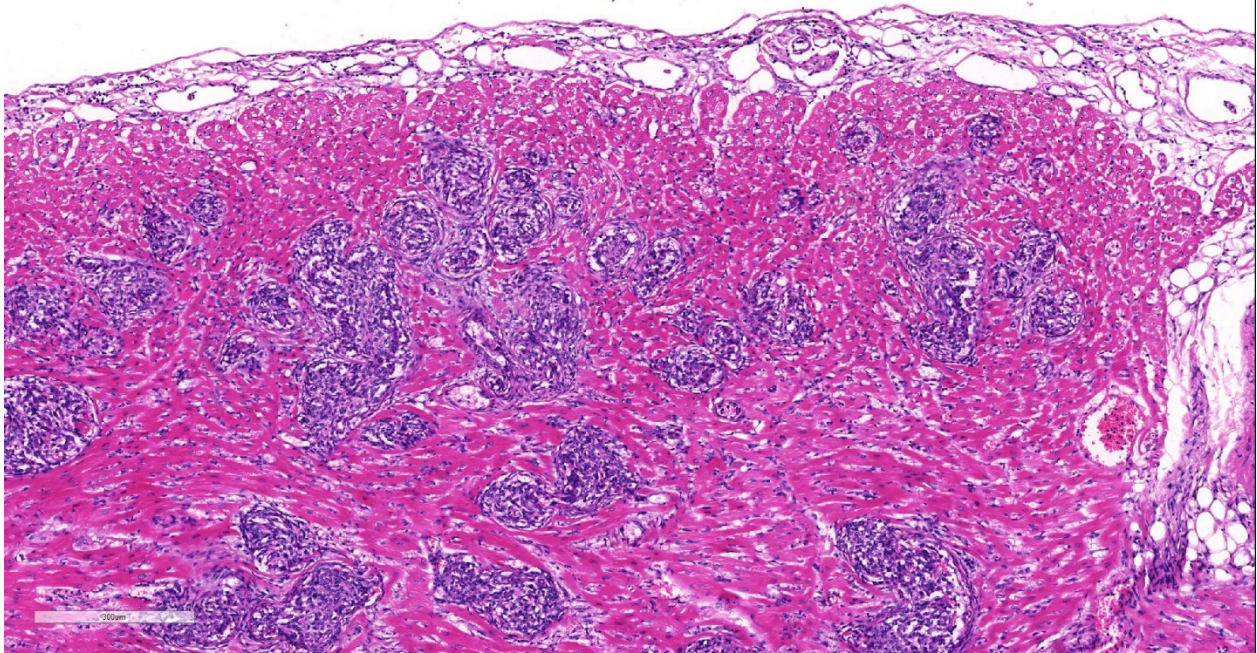
**Heart, cat:** (HE, 5X) Areas of hypercellularity outline the distribution of myocardial vessels within the outer half of the left ventricle, interventricular septum, and right ventricular wall (HE, 7X)

shortly after respiratory and cardiac arrest ensued. The owners decided for the resuscitation procedure to be interrupted.

**Gross Pathology:** The animal was in fairly good general condition with considerable visceral deposits of adipose tissue. Within the pleural cavity there were approximately 50 ml of reddish fluid. Moderate amount of pinkish fluid is present within the trachea and extend to the bifurcation and bronchi. Multifocal areas of collapse are noted affecting multiple pulmonary lobes. Within the pericardial cavity there was a small amount (less than 10 ml) of reddish fluid. Thin fibrin tags were noted on the surface of the left atrium, and few 2x3 mm irregular areas of dark red discoloration were present on the epicardium in the upper portion of the left ventricle. The heart appeared moderately elongated and enlarged, and weighed 20.44 gr. The heart was fixed whole and re-evaluated a few days after fixation. Multiple transverse sections in the mid to lower portion of the ventricles were taken. The left ventricular wall and interventricular septum appeared moderately thickened with substantial reduction of the left ventricle lumen.

The spleen was moderately enlarged. The femoral bone marrow was diffusely plum red in color. In the urinary bladder there were multifocal ectatic venous vessels visible from the mucosal surface.

**Laboratory results:** Hematology evaluation showed a haematocrit of 20.8%, mild leukocytosis with a normal neutrophil count and thrombocytopenia. A blood smear examination revealed moderate regeneration with polychromasia, anisocytosis and circulating red blood cell precursors. Testing for *Mycoplasma haemofelis* on a sample of peripheral blood was negative. There were some platelet aggregates on examination and



*Heart, cat: Arterioles are expanded by concentric to haphazard arrangement of spindle cells. (HE, 88X)*

on visual examination her platelet count was between  $45-60 \times 10^9/I$ .

Clinical chemistry revealed a mild azotemia, increases in ALT (290U/I) and AST (219U/I) and a mild increase in total bilirubin.

Slide agglutination test was unremarkable and Coombs test was negative.

#### **Microscopic Description:**

Involving approximately 30-40% of the tissue within the myocardium of the left and right ventricle and interventricular septum, there are proliferative changes multifocally affecting small to medium sized vessels. The vascular changes are characterised by proliferation of haphazardly arranged spindle cells frequently delimiting small slit-like spaces frequently showing the presence of erythrocytes and occasional fibrin thrombi. Some proliferations, characterised by a round shape and irregularly anastomosed vascular spaces, are reminiscent of glomeruloid structures. Multifocal variably sized areas of

oedema with separation and disruption of cardiomyocytes are detectable, in some instances characterised by accumulation of small numbers of extravasated erythrocytes (microhaemorrhages). Scattered foci or small areas of cardiomyocyte condensation, shrinkage and fragmentation (degeneration and necrosis) are detectable with some variation among the sections. Focal areas of myocardial and subendocardial haemorrhage affecting a portion of a papillary muscle of the left ventricle are noted (but not present in all sections). Numerous small infiltrates of moderate numbers of lymphocytes, plasma cells and few macrophages are noted multifocally along the epicardium.

The plump spindloid cells comprising the vascular proliferative lesions were characterised by consistent moderate to strong cytoplasmic immunoreactivity for alpha smooth muscle actin (aSMA) and only occasional positive staining for van Willebrand Factor (vWF). On the other hand, strong vWF immunolabeling was consistently observed in fibrin and platelet thrombi associated with the small irregular



and slit-like lumens of the vascular proliferative lesions.

Vascular proliferative changes similar to those observed in the heart were also noted in the spleen, in the bone marrow, and in the kidney, affecting the afferent arterioles at the vascular pole of the glomeruli, and to variable extents the of glomerular tuft capillaries.

**Contributor's Morphologic Diagnoses:**

Heart, intravascular endothelial and pericyte proliferation, marked, multifocal, consistent with reactive angioendotheliomatosis

**Contributor's Comment:**

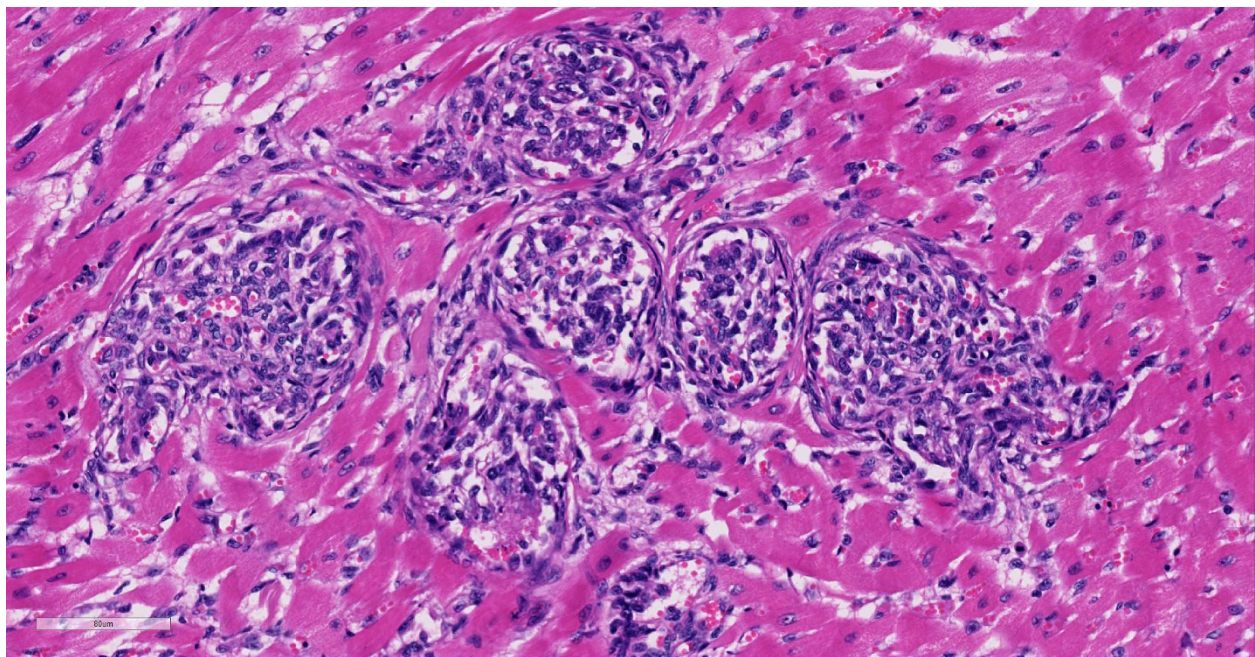
The term "angioendotheliomatosis" in human medicine has been a subject of controversy and confusion, resolved with the recognition of two distinct conditions:

"malignant angioendotheliomatosis" form representing a type of aggressive intravascular lymphoma, and "reactive angioendotheliomatosis" (RAE) which

consists of endothelial cells and pericyte proliferation. 15 proliferative changes mainly affecting small to medium sized vessels of the skin. Notably, two cases of intravascular disseminated angiosarcoma were also reported in humans and discussed as examples of "true neoplastic angioendotheliomatosis".<sup>8</sup>

Seventeen cases of "malignant angioendotheliomatosis" (intravascular lymphoma) were described in the dog, with consistent involvement of the central nervous system and variable involvement of other tissues,<sup>9</sup> and a single case was described in the cat.<sup>6</sup> Sporadic cases of feline multisystemic disease characterized by vascular endothelial and pericyte proliferative lesions have been reported, addressing comparisons with different vasoproliferative conditions in humans and other animal species.<sup>4,11,12</sup>

A subsequent report describing a case series of cats affected by similar multisystemic



*Heart, cat: Higher magnification of affected vessels. Slit-like lumina containing erythrocytes are present between spindle cells, and dilated vessels compress adjacent hyalinized cardiomyocytes. (HE, 278X)*

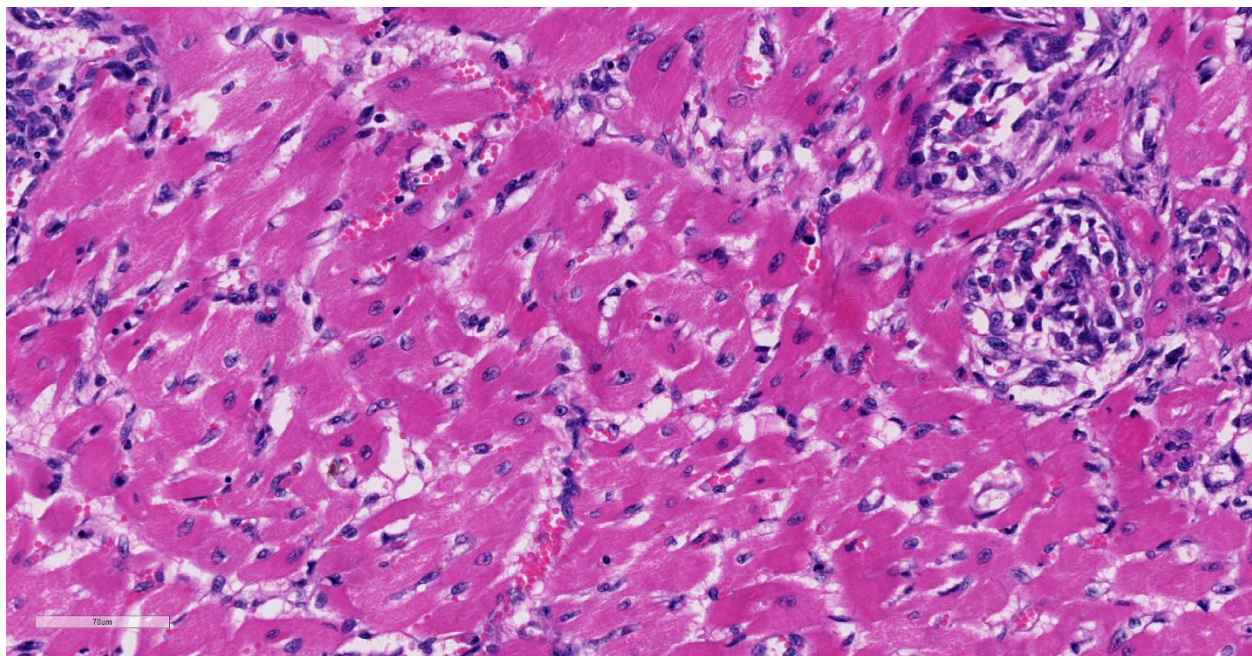
vascular proliferative lesions and addressing a review of the literature, defined the criteria for the classification of this condition as feline systemic reactive angioendotheliomatosis.<sup>5</sup> This rare condition in cats proves invariably fatal and frequently characterized by cardiac dysfunction and/or failure, variably associated with respiratory distress, in some cases hematological alterations. Serosanguinous and/or fibrinous pericardial effusions were reported in some instances, similar to those observed in our case. Microscopic evidence of vascular proliferative changes was most consistently observed in the heart in all cases. Spleen, kidney and lymph nodes were also frequently involved. Other organs affected at lower frequency included pancreas, gastrointestinal tract, brain, meninges, eyes, adrenals, spinal cord, liver, subcutis, thyroids, sciatic nerve and bone marrow.<sup>4-5,11-12</sup>

The etiopathogenesis of reactive angioendotheliomatosis remains obscure in both humans and cats. The possible

association of reactive angioendotheliomatosis with underlying infection, thrombotic thrombocytopenic purpura (TTP), autoimmune disorders, hypersensitivity, cryoglobulinemia, renal and liver failure, post liver transplantation, bone marrow transplantation-related graft versus host disease has been discussed in humans<sup>7,10,15</sup>

A recent report described the detection of DNA of different *Bartonella* species, including *B. vinsonii* subsp. *berkhoffii*, *B. henselae*, and *B. koehlerae* from tissues of cats affected by systemic reactive angioendotheliomatosis.<sup>1</sup> The authors also provide evidence for *B. vinsonii* subsp. *berkhoffii* causing upregulation of hypoxia inducible factor-1 a (HIF-1 a) with resulting increased production of vascular endothelial growth factor (VEGF) in an *in vitro* cell culture system.<sup>1</sup>

Lesions with features strikingly similar to feline systemic reactive angioendotheliomatosis were reported in a 2-year

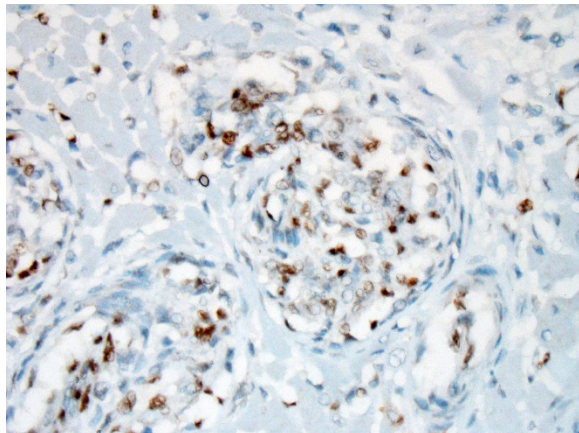


*Heart, cat: Cardiomyocytes adjacent to affected arterioles often show evidence of degeneration (hyalinization and loss of cross striations) and necrosis (pyknosis). (HE, 317X)*



old steer presumed to be persistently infected with bovine viral diarrhea virus (BVDV). BVDV antigen was detected in a proportion of the glomeruloid intravascular proliferations.<sup>3</sup> The authors addressed a possible comparison between the multisystemic vascular proliferative changes and a TTP-like condition ensuing in the animal. The possibility of relationship between BVDV infection and the development of the intravascular proliferative lesions was also discussed although a causal connection could not be definitively demonstrated.<sup>3</sup> Interestingly, tissue samples from this animal were also submitted for molecular analysis and *B. henselae* DNA was isolated from the vascular proliferative lesions affecting that steer.<sup>1</sup> These results offer interesting perspectives on the postulated association between infection with *Bartonella* spp. and the development of vascular proliferative changes including bacillary angiomatosis,<sup>16</sup> epithelioid haemangioendothelioma,<sup>2</sup> and hemangiosarcoma.<sup>2</sup>

However, a later study demonstrated that, in the context of diagnostic histopathology laboratories, multiple potential sources of cross-contamination associated with tissue



*Heart, cat: A portion of cells within the arteriolar lumina demonstrate strong nuclear immunopositivity for ERG transcription factor) (anti-ERG, 400X)*

processing may result in *Bartonella* spp. DNA carryover and need to be carefully monitored and excluded to ensure the validity and significance of *Bartonella* spp. isolation from paraffin embedded tissues.<sup>13</sup>

Immunohistochemical labeling performed at the JPC showed that some of the proliferative cells within the arterioles were positive for smooth muscle actin, while a second population within the proliferative masses were simultaneous immunopositive for Factor VIII antigen as well as ERG transcription factor.

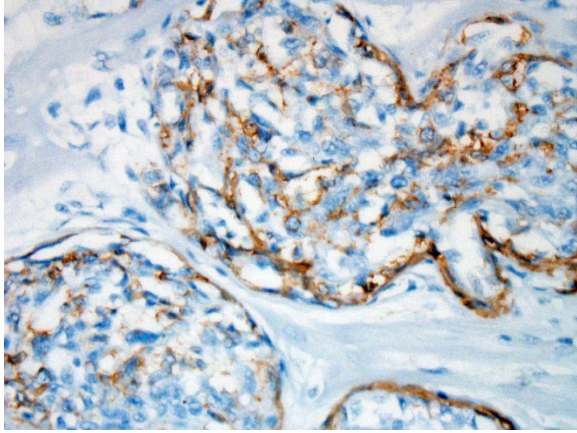
**Contributing Institution:**

Veterinary Diagnostic Services, School of Veterinary Medicine  
College of Medical, Veterinary and Life Sciences, University of Glasgow  
Bearsden Road  
G61 1QH  
Glasgow, United Kingdom  
[www.glasgow.ac.uk/vds](http://www.glasgow.ac.uk/vds)

**JPC Diagnosis:** Heart arterioles: Atypical endothelial and pericyte proliferation (angioendotheliomatosis), diffuse, severe, with cardiomyocyte degeneration, necrosis, and myocardial fibrosis.

**JPC Comment:** The contributor excellently summarizes the available literature on this rare condition of cats. Since 1985, the veterinary literature is limited to a total of 15 cases, not including two WSC submissions during this time (WSC 2008 Conf. 3 Case 2 and WSC 2014 Conf. 21, Case 3). Since the submission of this case, a single case report was published on this particular entity.<sup>17</sup> Immunohistochemical results for this condition have been published in several articles on this condition in the cat,<sup>5,11,17</sup> with intraluminal spindle cells staining strongly positive for Factor-VIII related antigen and VWF, and occasionally for smooth muscle





*Heart, cat: A portion of cells within the arteriolar lumina demonstrate strong cytoplasmic immunoreactivity for smooth muscle actin. (anti-SMA, 400X)*

actin (suggesting that some of the cells within the proliferation are of pericyte origin.) Immunohistochemical stains for FVIIIra and smooth muscle actin run at the JPC are in agreement with these findings. Because of the dual cell population, lesions of FSRA are considered to be an aberrant reactive process rather than a neoplasm.

The contributor also points out potential confusion in the naming of this particular condition. A very different condition, intravascular lymphoma, is presented in the veterinary literature as “malignant angioendotheliomatosis” (aka “intravascular lymphomatosis” and “angiotropic large-cell lymphoma”). While the syndrome of FRSA does bear a similar morphology to the human disease of reactive endotheliomatosis (which in humans is restricted to the skin), there does not appear to be a human precedent for the unfortunate name of “malignant angioendotheliomatosis.”

#### References:

1. Beerlage C, Varanat M, Linder K, Maggi RG, Cooley J, Kempf VA, Breitschwerdt EB. Bartonella vinsonii subsp. berkhoffii and Bartonella henselae as potential causes of proliferative vascular

- diseases in animals. *Med Microbiol Immunol.* 2012; 201(3): 319- 326.
2. Breitschwerdt EB, Maggi RG, Varanat M, Linder KE, Weinberg G. Isolation of Bartonella vinsonii subsp. berkhoffii genotype II from a boy with epithelioid hemangioendothelioma and a dog with hemangiopericytoma. *J Clin Microbiol.* 2009; 47 (6): 1957-1960.
3. Breshears MA, Johnson BJ. Systemic reactive angioendotheliomatosis-like syndrome in a steer presumed to be persistently infected with bovine viral diarrhea virus. *Vet Pathol.* 2008; 45 (5): 645-649.
4. Dunn KA, Smith KC, Blunden AS. Fatal multisystemic intravascular lesions in a cat. *Vet Rec.* 1997; 140(5): 128-129.
5. Fuji RN, Patton KM, Steinbach TJ, Schulman FY, Bradley GA, Brown TT, Wilson EA, Summers BA. Feline systemic reactive systemic angioendotheliomatosis: eight cases and literature review. *Vet Pathol.* 2005; 42(5): 608-617.
6. Lapointe JM, Higgins RJ, Kortz GD, Bailey CS, Moore PF. Intravascular malignant T-cell lymphoma (malignant angioendotheliomatosis) in a cat. *Vet Pathol.* 1997; 34(3): 247-250
7. Lazova R, Slater C, Scott G. Reactive angioendotheliomatosis. Case report and review of the literature. *Am J Dermatopathol.* 1996; 18 (1 ): 63-69.
8. Lin BT, Weiss LM, Battifora H. Intravascularly disseminated angiosarcoma: true neoplastic angioendotheliomatosis? Report of two cases. *Am J Surg Pathol.* 1997 21(10): 1138-1143.

9. McDonough SP, Van Winkle TJ, Valentine BA, vanGessel YA, Summers BA. Clinicopathological and immunophenotypical features of canine intravascular lymphoma (malignant angioendotheliomatosis). *J Comp Pathol.* 2002; 126 (4): 277-288.
  10. McMenamin ME, Fletcher CD. Reactive angioendotheliomatosis: a study of 15 cases demonstrating a wide clinicopathologic spectrum. *Am J Surg Pathol.* 2002; 26 (6): 685-697.
  11. Rothwell TL, Xu FN, Wills EJ, Middleton DJ, Bow JL, Smith JS, Davies JS. Unusual multisystemic vascular lesions in a cat. *Vet Pathol.* 1985; 22(5): 510-512.
  12. Straumann Kunz U, Ossent P, Lott-Stolz G. Generalized intravascular proliferation in two cats: endotheliosis or intravascular pseudoangiosarcoma? *J Comp Pathol.* 1993; 109 (1): 99-102.
  13. Varanat M, Maggi RG, Linder KE, Horton S, Breitschwerdt EB. Cross-contamination in the molecular detection of Bartonella from paraffin-embedded tissues. *Vet Pathol.* 2009; 46 (5): 940-944.
  14. Varanat M, Maggi RG, Linder KE, Breitschwerdt EB. Molecular prevalence of Bartonella, Babesia and hemotropic Mycoplasma sp. in dogs with splenic disease. *J Vet Intern Med.* 2011; 25 (6): 1284-1291
  15. Wick MR, Rocamora A. Reactive and malignant "angioendotheliomatosis": a discriminant clinicopathological study. *J Cutan Pathol.* 1988; 15 (5): 260-271.
  16. Yager JA, Best SJ, Maggi RG, Varanat M, Znajda N, Breitschwerdt EB. Bacillary angiomatosis in an immunosuppressed dog. *Vet Dermatol.* 2010; 21 (4): 420-428
- Yamamoto S, Shimoyana Y, Haruyama T. A case of feline systemic reactive angioendotheliomatosis. *J Fel Med Surg* 2015; doi: 10.1177/2044116915579684.